ORIGINAL PAPER

Electrochemical study of the thermodynamics and kinetics of hydrophilic ion transfers across water | *n*-octanol interface

François Quentel · Valentin Mirčeski · Maurice L'Her

Abstract Thermodynamics and kinetics of hydrophilic ion transfers across water|*n*-octanol (W|OCT) interface have been electrochemically studied by means of novel three-phase and thin-film electrodes. Three-phase electrodes used for thermodynamics measurements comprise edge plane pyrolytic graphite, the surface of which was partly modified with an ultrathin film of OCT, containing hydrophobic lutetium bis(tetra-*tert*-butylphthalocyaninato) (Lu[*t*Bu$_4$Pc]$_2$) as a redox probe. The transfers of anions and cations from W to OCT were electrochemically driven by reversible redox transformations of Lu[*t*Bu$_4$Pc]$_2$ to chemically stable lipophilic monovalent cation $\left(\text{Lu[}t\text{Bu}_4\text{Pc]}_2^+\right)$ and anion (Lu[*t*Bu$_4$Pc]$_2^-$), respectively. Upon reduction of Lu[*t*Bu$_4$Pc]$_2$, the transfers of alkali metal cations from W to OCT have been studied for the first time, enabling estimation of their Gibbs transfer energies. For kinetic measurements, a thin-film electrode configuration has been used, consisting of the same electrode covered completely with a thin layer of OCT that contained the redox probe and a suitable electrolyte. Combining the fast and sensitive square-wave voltammetry with thin-film electrodes, the kinetics of ClO_4^-, NO_3^-, and Cl^- transfers have been estimated.

F. Quentel · M. L'Her
Laboratoire de Chimie Analytique, UMR-CNRS 6521,
Université de Bretagne Occidentale,
6, avenue Victor Le Gorgeu, C.S. 93837,
29238 Brest Cedex 3, France

V. Mirčeski (✉)
Institute of Chemistry, Faculty of Natural Sciences
and Mathematics, University "Ss Cyril and Methodius",
P.O. Box 162, 1000 Skopje, Republic of Macedonia
e-mail: valentin@iunona.pmf.ukim.edu.mk

Introduction

Lipophilicity is one of the most critical parameters for fore-seeing a variety of physiological effects such as permeation through living cell membranes, binding affinity to biological receptors and enzymes, and toxicity [1]. For these reasons, lipophilicity is frequently exploited in various areas of chemistry, pharmacology, physiology, and medicine. Lipophilicity of a substance is quantitatively represented by the partition coefficient, P, referring to particular water-organic solvent biphasic system defined as $P = \exp\left(-\frac{\Delta^{w\rightarrow o}G^\theta}{RT}\right)$, where $\Delta^{w\rightarrow o}G^\theta$ is the standard Gibbs energy of transfer of the substance from water (W) to the organic solvent (O). Among various biphasic systems, water–*n*-octanol (W–OCT) is of exceptional importance [2]. Indeed, it became a standard system for determination of lipophilicity of substances due to the excellent correlation of the W–OCT partition coefficient (P_{OCT}) with the permeation ability of substances across the cell membranes [1]. In pharmacology, P_{OCT} is one of the critical descriptors in the quantitative structure–activity relationships [3]. This follows from the amphiphilic properties of OCT and its superficial similarities with lipids; it possesses a long alkyl hydrophobic chain and a hydrophilic hydroxyl group having electron-donating properties and being capable for hydrogen bonding.

Whereas various methods are available for determination of partition coefficients of uncharged species, measurements of the ion transfer energy are yet state of the art. Measurements based on potentiometry in a biphasic system, or classical shake-flask methods, provide only apparent partition coefficients of ionic species, being strongly dependent on the experimental conditions. When charged species are transferred across a liquid|liquid interface (L|L), electrochemical methods are the most suited ones for both

thermodynamics and kinetics measurements [4]. Unfortunately, the well-established voltammetric methods based on the four-electrode arrangement at the interface between two immiscible electrolyte solutions are inapplicable to the W| OCT system [4]. Only recently, a new experimental strategy has been developed to access the ion transfer reactions at the W|OCT interface by using three-phase electrodes [5]. The latter electrode system, consisting of a paraffin-impregnated graphite electrode modified with a macroscopic droplet of an organic solvent containing a neutral redox probe, is simple, but powerful tool to measure thermodynamics of ion transfer reactions [6–10]. Scholz et al. showed recently that the three-phase electrode consisting of a paraffin-impregnated graphite electrode modified with a droplet of *n*-octanol containing decamethylferrocene (DMFC) as a redox probe can be utilized to measure the Gibbs energies of monovalent anion transfer from water to *n*-octanol [5]. Later on, the same method has been utilized to determine the octanol partition coefficients of a large series of organic compounds with a potential pharmacological activity [9]. Moreover, using octan-2-ol as a chiral solvent and chiral anions, the effect of chirality on the transfer energies has been addressed [11].

The capabilities of the three-phase electrodes to assess the thermodynamics of the ion transfer reactions across the L|L interface depend strongly on the type of the redox probe used [12, 13]. When DMFC is used as a redox probe, the three-phase electrodes are mainly restricted to the anion transfer reactions. In the present study, a novel three-phase electrode is presented, with superior features compared to the previous ones, enabling inspection of both anion and cation transfer reactions across W|OCT interface. The present three-phase electrode consists of an edge plane pyrolytic graphite electrode (EPPGE) modified with a very thin film of *n*-octanol solution containing lutetium bis(tetra-*tert*-butylphthalocyaninato) ($Lu[tBu_4Pc]_2$) as a redox probe (Scheme 1). As $Lu[tBu_4Pc]_2$ can be both oxidized and reduced to a stable lipophilic monovalent cation and anion, respectively, the transfers of anions and cations across W| OCT interface can be simultaneously inspected [12]. To the best of our knowledge, the present communication reports on a first set of electrochemical experiments of the transfer of strongly hydrophilic cations from water to *n*-octanol. The experiments provide evidences for appreciably low energies for transfer from water to *n*-octanol of alkali metal cations such as Li^+, Na^+, K^+, and Rb^+, implying a strong coordinating affinity of *n*-octanol toward these cations. A comparative analysis between water–*n*-octanol and water–nitrobenzene (W–NB) systems reveals that octanol facilitates the cation transfer reactions lowering significantly the transfer energy. Finally, we demonstrate for the first time that the EPPGE modified with a thin film of *n*-octanol in combination with square-wave voltammetry (SWV) can be
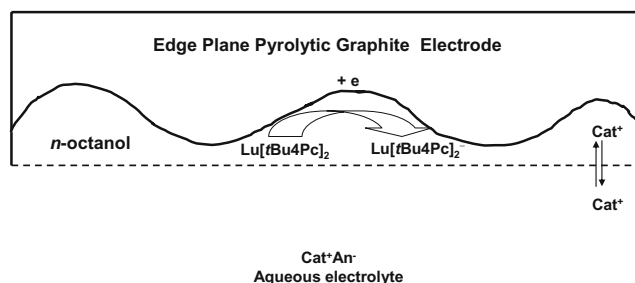
Scheme 1 Schematic representation of the three-phase electrode, showing the possible microstructure of a part of the EPPGE covered with an uneven film of *n*-octanol that contains $Lu[tBu_4Pc]_2$ as redox probe

successfully applied to inspect the kinetics of anion transfers across W|OCT interface [14–16].

Experimental

$Lu[tBu_4Pc]_2$ was synthesized and purified according to the procedure already described [17, 18]. All other chemicals were of high purity and used as received. $Lu[tBu_4Pc]_2$ was dissolved in water-saturated octan-1-ol (*n*-octanol) or nitrobenzene at concentration of 1.4 mmol/l.

A disk electrode (0.32 cm²) of edge plane highly oriented pyrolytic graphite has been used. The preparation and pretreatment of the electrode is described elsewhere [14]. The organic solutions were deposited on the graphite electrode with the help of a micropipette. Both *n*-octanol and nitrobenzene solution spread spontaneously over the electrode surface. For the thermodynamic measurements (see "Thermodynamics of ion transfers across water|*n*-octanol interface"), 0.2 μl of the organic solution was deposited on the electrode surface. Such a minute volume of the organic solution does not cover completely the electrode surface, thus forming a three-phase boundary line after immersing the electrode into the aqueous phase [13].

For kinetic measurements of ClO_4^-, NO_3^-, and Cl^- transfers (see "Kinetics of Cl^-, NO_3^-, and ClO_4^- transfers across water|n-octanol interface"), a thin-film electrode configuration has been used (Scheme 2). The thin-film electrode was assembled by depositing 1 μl of the organic solvent covering completely the electrode surface. In this configuration, besides the redox probe, the organic phase contained a suitable electrolyte at concentration 0.1 mol/l. The electrolyte was $(C_4H_9)_4NClO_4$, $(C_4H_9)_4NNO_3$, and $(C_6H_{13})_4NCl$ for the transfer of ClO_4^-, NO_3^-, and Cl^-, respectively.

Voltammetric experiments have been conducted with SWV and cyclic voltammetry (CV) using an AUTOLAB equipment (Eco-Chemie, Utrecht, The Netherlands). A saturated calomel electrode or Ag/AgCl (sat. KCl) was used as reference and a platinum wire as auxiliary electrode.

Scheme 2 Schematic representation of the thin-film electrode consisting of EPPGE covered completely with a microfilm of *n*-octanol containing Lu[*t*Bu$_4$Pc]$_2$ as a redox probe and a suitable electrolyte
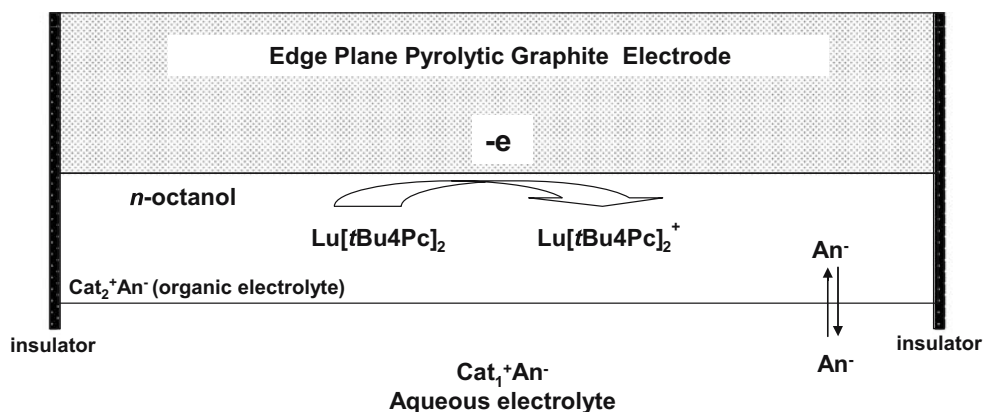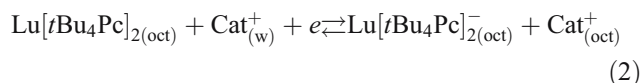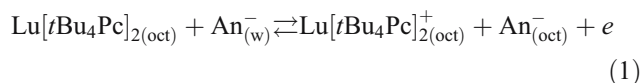

Water (Millipore Q) was saturated with *n*-octanol or nitrobenzene to prevent dissolution of the organic solvent in the aqueous phase.

Results and discussion

Thermodynamics of ion transfers across water|*n*-octanol interface

SW voltammograms recorded with the three-phase electrode in contact with various aqueous electrolytes are given in Fig. 1. The redox probe used, Lu[*t*Bu$_4$Pc]$_2$, can be oxidized and reduced in *n*-octanol, in one-electron reversible step, to form stable cation and anion, respectively. The peak at more positive potentials represents the oxidation of Lu[*t*Bu$_4$Pc]$_2$ to Lu[*t*Bu$_4$Pc]$_2^+$, whereas the peak at more negative potentials is due to reduction in Lu[*t*Bu$_4$Pc]$_2$ to

Fig. 1 Net SW voltammograms recorded with three-phase electrodes in contact with 0.5 mol/l NaCl, KNO$_3$, and LiClO$_4$ aqueous solutions. The three-phase electrodes were prepared by imposing 0.2 μl of *n*-octanol solution containing 1.4 mmol/l Lu[*t*Bu$_4$Pc]$_2$. The parameters of the potential modulation were: frequency *f*=50 Hz, amplitude E_{sw}= 50 mV, and potential increment d*E*=0.1 mV
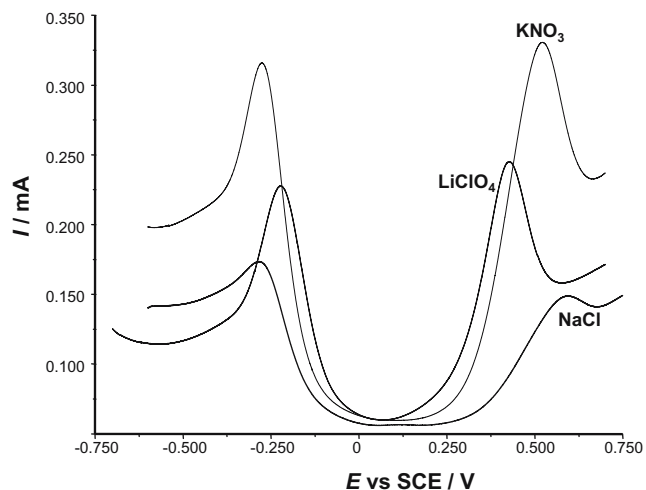
Lu[*t*Bu$_4$Pc]$_2^-$. Both the cation and anion of the redox probe are strongly lipophilic, being confined within the organic phase. Thus, to preserve the electroneutrality of the organic phase, the electrode reactions of the redox probe are accompanied by a simultaneous transfer of corresponding ions from water to *n*-octanol. As a consequence, the formal potentials of the overall electrochemical processes are dependent on the nature and concentration of the aqueous electrolyte, reflecting the energy required to drive the ion transfer at the OCT|W interfaces. The overall electrochemical processes for the oxidation and reduction processes are described by the following coupled electron-ion transfer reactions 1 and 2, respectively:

$$\text{Lu}[t\text{Bu}_4\text{Pc}]_{2(\text{oct})} + \text{An}^-_{(\text{w})} \rightleftarrows \text{Lu}[t\text{Bu}_4\text{Pc}]^+_{2(\text{oct})} + \text{An}^-_{(\text{oct})} + e \tag{1}$$

$$\text{Lu}[t\text{Bu}_4\text{Pc}]_{2(\text{oct})} + \text{Cat}^+_{(\text{w})} + e \rightleftarrows \text{Lu}[t\text{Bu}_4\text{Pc}]^-_{2(\text{oct})} + \text{Cat}^+_{(\text{oct})} \tag{2}$$

When the concentration of the redox probe is significantly lower than the concentration of the transferring ion, the formal potential of the oxidation process 1 at the three-phase electrode is given by [6]:

$$E_c^{\theta\prime} = E^{\theta}_{\text{Lu}[t\text{Bu}_4\text{Pc}]^+_{2(\text{oct})}|\text{Lu}[t\text{Bu}_4\text{Pc}]_{2(\text{oct})}} + \Delta^{\text{w}\rightarrow\text{oct}}\phi^{\theta}_{\text{An}^-}$$
$$- \frac{RT}{F}\ln\left(a_{\text{An}^-(\text{w})}\right) + \frac{RT}{F}\ln\left(\frac{a^*_{\text{Lu}[t\text{Bu}_4\text{Pc}]_{2(\text{oct})}}}{2}\right) \tag{3}$$

where $E^{\theta}_{\text{Lu}[t\text{Bu}_4\text{Pc}]^+_{2(\text{oct})}|\text{Lu}[t\text{Bu}_4\text{Pc}]_{2(\text{oct})}}$ is the standard potential of the Lu[*t*Bu$_4$Pc]$_2$/Lu[*t*Bu$_4$Pc]$_2^+$ redox couple in *n*-octanol, $\Delta^{\text{w}\rightarrow\text{oct}}\phi^{\theta}_{\text{An}^-}$ being the standard potential for the transfer of An$^-$ from water to *n*-octanol, $a^*_{\text{Lu}[t\text{Bu}_4\text{Pc}]_{2(\text{oct})}}$ is the activity of the redox probe in the bulk of the organic phase, and the other symbols have their usual meaning. Notice that the standard potential of the ion transfer is related to the standard Gibbs energy $\Delta^{\text{w}\rightarrow\text{oct}}G^{\theta}_{\bar{F}}$ through $\Delta^{\text{w}\rightarrow\text{oct}}\phi^{\theta}_{\bar{F}} = -\frac{\Delta^{\text{w}\rightarrow\text{oct}}G^{\theta}_{\bar{F}}}{zF}$,

where z is the charge of the transferring ion, i. The formal potential of the electrochemical reaction 2 is given by [19]:

$$E_c^{\theta'} = E^{\theta}_{Lu[tBu_4Pc]_{2(oct)}|Lu[tBu_4Pc]]^-_{2(oct)}} + \Delta^{w \rightarrow oct}\phi^{\theta}_{Cat^+}$$

$$+ \frac{RT}{F}\ln\left(a_{Cat^+_{(w)}}\right) - \frac{RT}{F}\ln\left(\frac{a^*_{Lu[tBu_4Pc]_{2(oct)}}}{2}\right) \qquad (4)$$

Equations 3 and 4 predict the formal potentials to be dependent on the type of the transferring ion. Note that the net SW peak potential is equivalent to the formal potential for a reversible electrochemical process [20]. Hence, the results presented in Fig. 1 confirm the prediction of Eqs. 3 and 4. The relative position of the oxidation peak, corresponding to the transfer of ClO_4^-, NO_3^-, and Cl^-, correlates with the hydrophilicity of the transferring anions. The overall energy required for the oxidation process increases in proportion to the hydrophilicity of the transferring anion, causing the oxidation peak to shift toward more positive potentials (Fig. 1). However, the position of the reduction peak does not correlate with the hydrophilicity of the transferring cations (Li^+, Na^+, and K^+). Based on the hydration energy of the transferring cation, it is expected of the overall energy for the reduction process to increase in the order $K^+ < Na^+ < Li^+$. However, the results given in Fig. 1 show an opposite trend.

As indicated by Eqs. 3 and 4, to determine the standard potential of the ion transfer, the measurements of the formal potential together with the knowledge of the standard potential of the redox couples in n-octanol are required. Determination of the standard redox potential can be done only on the basis of an extrathermodynamic assumption, such as Strehlow [21] or tetraphenylarsonium tetraphenylborate (TPATPB) assumption [4]. Application of the Strehlow assumption requires considering the standard potential of the ferrocenium/ferrocene couple as being identical in all the solvents and in aqueous solution. An attempt to measure the standard potentials of $Lu[tBu_4Pc]_2^+/Lu[tBu_4Pc]_2$ and $Lu[tBu_4Pc]_2/Lu[tBu_4Pc]_2^-$ redox couples vs ferrocene in n-octanol was unsuccessful, as the ferrocene oxidation did not provide reliable voltammetric results. An alternative approach is to calibrate the three-phase electrode using ions with known standard potentials of transfer across W|OCT interface determined on the basis of TPATPB assumption. To the best of our knowledge, no electrochemical data exist for energies of cation transfers from water to n-octanol. The only existing set of electrochemical data given in [5] refers to the transfer energies of Cl^-, ClO_4^-, NO_3^-, SCN^-, and BF_4^-. Using these data, the three-phase electrode was calibrated by measuring the formal potential for the oxidation of $Lu[tBu_4Pc]_2$ in the presence of various transferring anions. The calibration line is given in Fig. 2, showing the linear dependence between the net SW peak potential for the oxidation peak vs the standard potentials of
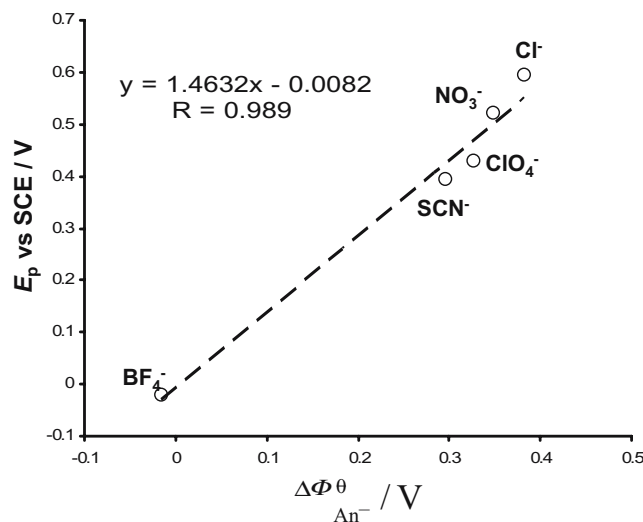

Fig. 2 Dependence of the oxidation net peak potentials of Lu[$tBu_4Pc]_2$ recorded at the three-phase electrode on the standard anion transfer potentials taken from [5]. All experimental conditions were the same as for Fig. 1

anion transfers. As implied by Eq. 3, the dependence $E_c^{\theta'}$ vs $\Delta^{w \rightarrow oct}\phi^{\theta}_{An^-}$ is a line with a slope equal to 1, which is in a fairly good agreement with the calibration line given in Fig. 2. Taking into account Eq. 3 and the slope of the calibration line, the standard potential of the $Lu[tBu_4Pc]_2^+/Lu[tBu_4Pc]_2$ in n-octanol was estimated as $E^{\theta}_{Lu[tBu_4Pc]^+_{2(oct)}|Lu[tBu_4Pc]_{2(oct)}} = 0.399$ V vs noram hydrogen electrode (NHE) (TPATPB assumption).

Having in hand the standard potential of the $Lu[tBu_4Pc]_2^+/Lu[tBu_4Pc]_2$ couple, the standard potential of $Lu[tBu_4Pc]_2/Lu[tBu_4Pc]_2^-$ can be determined by studying the electrochemistry of $Lu[tBu_4Pc]_2$ in the water-saturated solvent. For this purpose, conventional voltammetric measurements of $Lu[tBu_4Pc]_2$ have been conducted in n-octanol containing 0.1 mol/l $(C_4H_9)_4NNO_3$ as the supporting electrolyte and using EPPGE as a working electrode. A representative net SW voltammogram of such measurements is given in Fig. 3, showing a well-developed net voltammetric peaks for both oxidation and reduction processes of $Lu[tBu_4Pc]_2$ in n-octanol. From the difference in the peak potentials for the oxidation and reduction processes, (ΔE_p=0.450 V) the standard potential of the redox couple $Lu[tBu_4Pc]_2/Lu[tBu_4Pc]_2^-$ in n-octanol was estimated to be $E^{\theta}_{Lu[tBu_4Pc]_{2(oct)}|Lu[tBu_4Pc]^-_{2(oct)}} = -0.051$ V vs NHE. Recall that the redox potentials of the two redox couples are estimated on the basis of TPATPB extrathermodynamic assumption, as this was involved in the standard potentials of anion transfers used for the calibration line presented in Fig. 2.

Knowing $E^{\theta}_{Lu[tBu_4Pc]_{2(oct)}|Lu[tBu_4Pc]^-_{2(oct)}}$, and measuring the formal potential of the reduction peak at the three-phase electrode in contact with various electrolytes, the standard potentials of a series of cation transfers at the W|OCT
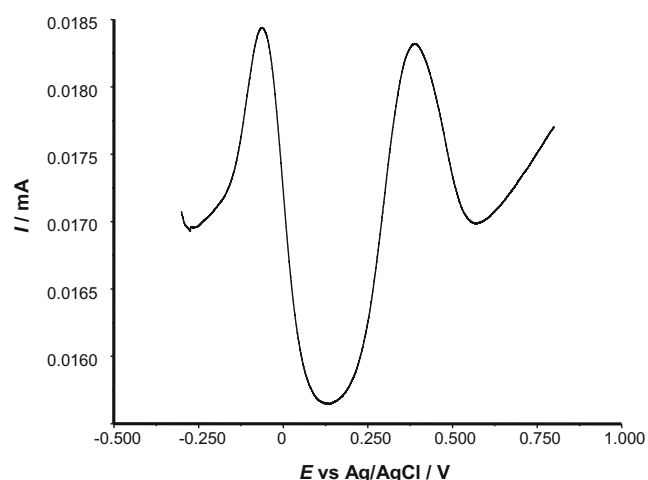
Fig. 3 SW voltammogram of 1.4 mmol/l Lu[tBu$_4$Pc]$_2$ solution in n-octanol containing 0.1 mol/l (C$_4$H$_9$)$_4$NNO$_3$ as a supporting electrolyte recorded at EPPGE. The frequency of the potential modulation was f= 8 Hz. The other conditions were the same as for Fig. 1

interface have been estimated. The results are summarized in Table 1. Interestingly, the affinity of alkali metal cation for n-octanol is much higher than for other solvents [22]. For the sake of comparison, the last column of Table 1 shows the corresponding energies for the transfers across W|NB interface. Considering the fact that the relative permittivity of n-octanol (ε=10.3) is lower than that of nitrobenzene (ε= 34.8), it is obvious that the long-range electrostatic interactions between n-octanol and alkali cations do not determine the energy of transfer, rather than specific short-range interactions (i.e., donor–acceptor effects), origination from the coordination affinity of hydroxyl group toward alkali metal cations, play a critical role. For instance, Li$^+$ is the most hydrophilic cation with respect to the W-NB system, whereas it is the most lipophilic regarding W-OCT system. This assumption is supported by the absence of the correlation between the estimated transfer energies and the crystallographic radius of the alkali metal cations. In the case of organic cations, such as (CH$_3$)$_4$N$^+$ and (C$_2$H$_5$)$_4$N$^+$, n-octanol does not exhibit coordination activity; hence, the

electrostatic interactions prevail over the short-range interactions. For these reasons, the energy of transfer of these organic cations from water to n-octanol is higher compared to nitrobenzene (see Table 1), being in agreement with the lower permittivity of n-octanol than nitrobenzene. In the case of alkali metal cations, it should be also considered that, according to Osakai et al. [23], the transfer of hydrophilic ions from water to an organic solvent takes place together with some water molecules associated with the ions, rather than through a mechanism involving dehydration in water and reformation of a new solvation sphere in the organic solvent. Therefore, as the solubility of water in n-octanol (2.4 mol/l) is significantly higher than in nitrobenzene (0.2 mol/l), it is reasonable to admit that the transfer of hydrophilic ions in n-octanol is more thermodynamically favorable than in nitrobenzene.

To provide additional experimental evidences for the coordination affinity of octanol toward alkali metal cations, supplementary experiments have been conducted at the three-phase electrode using nitrobenzene as an organic solvent containing a variable amount of n-octanol. Figure 4 shows the effect of increasing amount of octanol in nitrobenzene solution on the position of both the reduction and oxidation peaks of Lu[tBu$_4$Pc]$_2$ corresponding to the transfer of Li$^+$ and Br$^-$, respectively. Increasing the content of octanol in nitrobenzene from 0 to 50% (v/v) caused a dramatic decrease in the energy required for Li$^+$ transfer due to coordination affinity of n-octanol. On the contrary, the oxidation peak corresponding to the transfer of Br$^-$ is only slightly affected by the presence of n-octanol. The inset of Fig. 4 shows a linear dependence of the reductive peak potentials on the logarithm of the volumic ratio ϕ of n-octanol in nitrobenzene. These experiments confirm the strong affinity of octanol toward coordination of Li$^+$, facilitating its transfer across the W|NB interface. The plot of the reduction peak potential vs the logarithm of the octanol concentration in nitrobenzene is a line with a slope of 55 mV. Under these conditions, one should keep in mind

Table 1 Voltammetric and thermodynamic data of the cation transfers from water to n-octanol

Cations	E_{p}/V	$\Delta_{\mathrm{w}}^{\mathrm{oct}}\phi_{\mathrm{Cat}^+}^{\theta}\big/\mathrm{V}$	$\Delta^{\mathrm{w}\to\mathrm{oct}}G_{\mathrm{cat}^+}^{\theta}\big/\mathrm{kJ\ mol^{-1}}$	$\Delta^{\mathrm{w}\to\mathrm{nb}}G_{\mathrm{cat}^+}^{\theta}\big/\mathrm{kJ\ mol^{-1}}$
Rb$^+$	−0.298	−0.130	12.6	19
Cs$^+$	−0.308	−0.140	13.5	12
Na$^+$	−0.316	−0.148	14.3	30
Li$^+$	−0.28	−0.112	10.8	36
K$^+$	−0.324	−0.156	15.1	21
(C$_2$H$_5$)$_4$N$^+$	−0.131	0.036	−3.5	−6.4
(CH$_3$)$_4$N$^+$	−0.291	−0.123	11.9	2.9

The second column lists the peak potential values measured by reduction of Lu[tBu$_4$Pc]$_2$ at the three-phase electrode in contact with 0.1 mol/l aqueous solution of CatCl, where Cat$^+$ is the corresponding cation. The other experimental conditions are the same as for Fig. 1. For the sake of comparison, the last column lists the values of the standard Gibbs energy of cation transfers from water to nitrobenzene taken from literature [22].
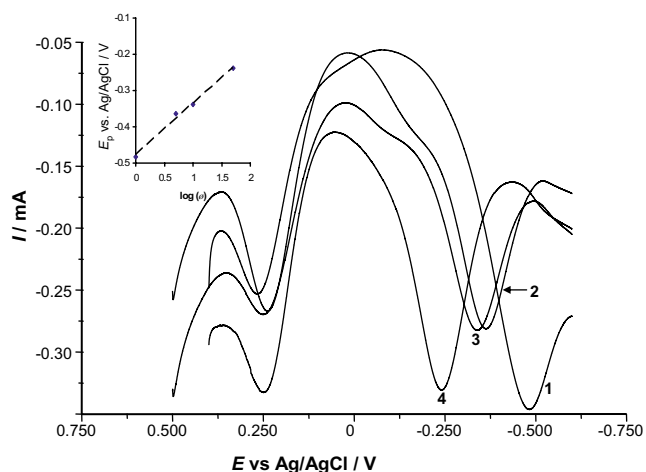
Fig. 4 Effect of *n*-octanol on the net SW voltammograms corresponding to the transfer of Li^+ (peak at more negative potentials) and Br^- (peak at more positive potentials) recorded by reduction and oxidation of $Lu[tBu_4Pc]_2$, respectively. The aqueous phase contains 1 mol/l LiBr. The three-phase electrode was prepared by spreading 0.2 μl of 1.4 mmol/l $Lu[tBu_4Pc]_2$ nitrobenzene/*n*-octanol solution. The content of *n*-octanol in nitrobenzene was: 0 (1), 5 (2), 10 (3), and 50% (4; *v/v*). All other conditions were the same as for Fig. 1. The *inset* shows the dependence of the reduction peak potentials on the logarithm of the volumic parts ϕ of *n*-octanol in nitrobenzene solution

that the acidity of octanol in a nitrobenzene solution is significantly higher compared to pure octanol. Thus, the electrostatic interactions between the ion and the octanol in a nitrobenzene solution are expected to be higher compared to the situation in a pure octanol.

Corresponding analysis to that presented in Fig. 4 has been performed for a series of other ions, and the results are summarized in Table 2. The second and the third columns list the peak potential values corresponding to the transfer from water to nitrobenzene and to a mixture of nitrobenzene and *n*-octanol (1:1 volumic parts), respectively. Note that, for cation and anion transfers, the reduction and oxidation peaks of $Lu[tBu_4Pc]_2$ have been exploited, respectively.

The fourth column gives the peak potential difference, and the last column lists the corresponding Gibbs energy change, calculated as $\Delta^{nb \rightarrow (nb+oct)}G_{ion^z}^\theta = -zF\Delta E_p$. The parameter $\Delta^{nb \rightarrow (nb+oct)}G_{ion^z}^\theta$ is the change of the Gibbs energy corresponding to the transfer of the ion from the nitrobenzene to the 1:1 mixture of nitrobenzene and *n*-octanol. Except for ClO_4^-, octanol has a higher affinity for the studied ions (Table 2). For the alkali metal cations, the effect is strongest for Li^+ and decreases for larger ions. Interestingly, there is an excellent correlation between $\Delta^{nb \rightarrow (nb+oct)}G_{ion^z}^\theta$ and ionic radius, as sketched by the curve 1 in Fig. 5. Moreover, curve 2 in Fig. 5 shows the same trend for the three studied anions. Only for ClO_4^-, $\Delta^{nb \rightarrow (nb+oct)}G_{ion^z}^\theta$ is positive, showing that the transfer of this ion from nitrobenzene to the nitrobenzene–*n*-octanol mixture is thermodynamically unfavorable. This is in agreement with the difference of the Gibbs energy of the ion transfer across W|NB interface ($\Delta^{w \rightarrow nb}G_{ClO_4^-}^\theta = 7.7$ kJ mol^{-1}) [22] and W|OCT interface ($\Delta^{w \rightarrow oct}G_{ClO_4^-}^\theta = 31.53$ kJ mol^{-1}) [5].

Kinetics of Cl^-, NO_3^-, and ClO_4^- transfers across water|*n*-octanol interface

Thin-film electrodes [14–16] in combination with SWV can provide kinetic information on the ion transfer reactions. The experimental strategy is based on the recently developed method known as a "quasireversible maximum" in thin-film voltammetry [24]. From an experimental point of view, the method is rather simple, requiring inspection of the net SW peak current by variation of the time-window of the voltammetric experiment, represented by the frequency of the potential modulation [20]. The theoretical background of the method has been elaborated in previous studies [15, 16].

In thin-film voltammetry, the ratio of the net peak current and the square root of the frequency ($\Delta I_p f^{-0.5}$, i.e.,

Table 2 Peak potentials measured by three-phase electrode corresponding to the transfers of ions from water to nitrobenzene (second column) and a 1:1 (*v/v*) mixture of nitrobenzene and octanol (third column)

Ion	E_p (NB)/V	E_p/V (NB + OCT)	ΔE_p/V	$\Delta^{nb \rightarrow (nb+oct)}G_{ion^z}^\theta \big/ $ kJ mol^{-1}
Li^+	−0.482	−0.24	0.242	−23.3
Na^+	−0.457	−0.264	0.193	−18.6
K^+	−0.329	−0.288	0.041	−3.9
Rb^+	−0.35	−0.336	0.014	−1.3
Cl^-	0.373	0.292	−0.081	−7.8
Br^-	0.265	0.248	−0.017	−1.6
ClO_4^-	0.181	0.242	0.061	5.8

The fourth column shows the difference in the peak potentials [$\Delta E_p = E_p(OCT) - E_p(NB + OCT)$], and the last column reports the corresponding variation of the Gibbs energy of the ion transfer. The concentration of the ions in the aqueous phase was 1 mol/l and 0.1 mol/l for Rb^+ and ClO_4^-. All experimental conditions are the same as for Fig. 1.
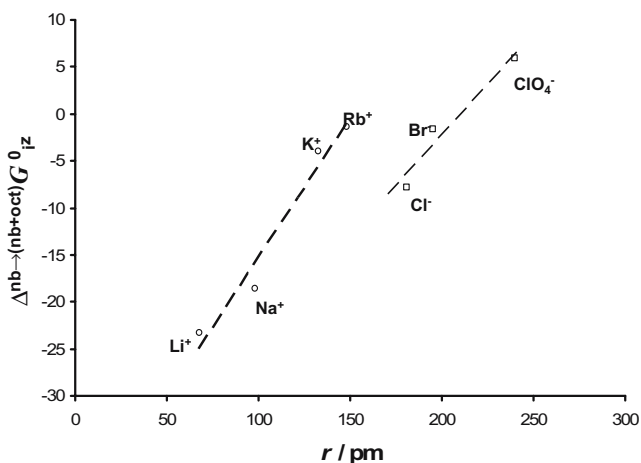
Fig. 5 The dependence of the Gibbs energy of transfer from nitrobenzene to the mixture of nitrobenzene and *n*-octanol (1:1 volumic ratio) on the radius of the transferring ion. All experimental data are the same as for Table 2

normalized net peak current) is a parabola-like function of the logarithm of the frequency. The parabolic function is attributed with a maximum, being positioned within the quasireversible kinetic region of the studied electrode reaction, thus termed as a "quasireversible maximum." As the position of the maximum is a function of the standard rate constant, it can be exploited for estimation of this essential kinetic parameter.

In thin-film voltammetry, the apparent kinetics of the electrode reaction is predominantly controlled by the dimensionless kinetic parameter $K = \frac{k_s}{\sqrt{Df}}$ that unifies the standard rate constant (k_s) with the common diffusion coefficient of the electroactive species (D) and the frequency of the potential modulation (f). The position of

the quasireversible maximum is associated with an exact critical value of the kinetic parameter K_{max}, which can be found by numerical simulations. In the experimental analysis, k_s and D are typical constants of a given experimental system, and only the frequency can be varied by the instrumentation. When the ratio $\frac{k_s}{\sqrt{Df}}$ is equal to the critical value of the kinetic parameter K_{max}, the normalized peak current $\Delta I_p f^{-0.5}$ reaches a maximal value. The frequency satisfying the condition $\frac{k_s}{\sqrt{Df}} = K_{max}$ is termed as a critical frequency, f_{max}. Therefore, measuring experimentally the critical frequency f_{max} and determining the critical kinetic parameter K_{max} with the help of numerical simulations [24], one can estimate the standard rate constant through the simple formula $k_s = K_{max}\sqrt{Df_{max}}$.

At the thin-film electrode sketched in Scheme 2, the overall electrochemical process couples the electron transfer at the EPPGE|OCT interface with the ion transfer at the OCT|W interface. Using Lu[tBu_4Pc]$_2$ as a redox probe, it has been shown that the ion transfer is the rate-determining step, at least considering the W|NB interface [14–16]. An important feature of the kinetic experiment performed with thin-film electrodes is the presence of an electrolyte in the organic phase. The first purpose of the electrolyte in the thin film is to minimize the ohmic-drop effect in the course of the voltammetric measurements [25]. Moreover, the electrolyte in the organic phase has a common ion with the aqueous electrolyte, which, at the same time, is the transferring ion. The concentration of the common ion is at least 100 times higher than that of the redox probe. As a consequence, the concentration of the transferring ion at the liquid interface is virtually constant in the course of the voltammetric experiment. Therefore, the common ion present in both liquid phases plays simultaneously two
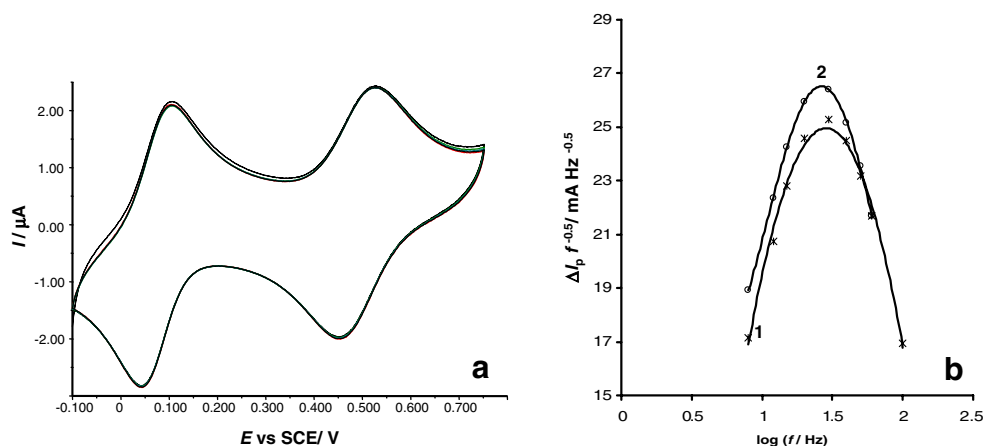
Fig. 6 **a** Repetitive cyclic voltammograms (five cycles) recorded with thin-film electrode in contact with 1 mol/l NaCl aqueous solution. **b** Quasireversible maxima corresponding to the transfer of Cl$^-$ measured by oxidation (*1*) and reduction (*2*) peak of Lu[tBu_4Pc]$_2$. The aqueous

phase contained 0.5 mol/l NaCl. For both **a** and **b**, the thin-film electrode was prepared by imposing 1 μl of the *n*-octanol solution containing 1.4 mmol/l Lu[tBu_4Pc]$_2$ and 0.1 mol/l (C$_6$H$_{13}$)$_4$NCl. The parameters of the potential modulation were the same as for Fig. 1
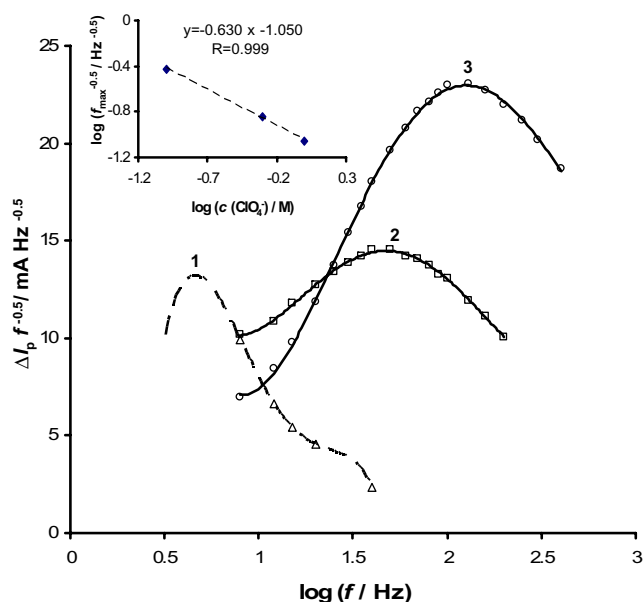
Fig. 7 The evolution of the quasireversible maxima with the concentration of the transferring ClO_4^- ions in the aqueous phase. The quasireversible maximum was measured by the oxidation of Lu[tBu$_4$Pc]$_2$. The concentration of the ClO_4^- in the aqueous phase was: 0.1 (1), 0.5 (2), and 1 mol/l (3). The cation in the aqueous phase was Li$^+$. The thin-film electrode was assembled by depositing 1-μl n-octanol solution containing 1.4 mmol/l Lu[tBu$_4$Pc]$_2$ and 0.1 mol/l (C$_4$H$_9$)$_4$NClO$_4$. The parameters of the potential modulation were the same as for Fig. 1

critical roles; it is the potential controlling ion of the L|L interface and the rate controlling ion of the overall electrochemical process at the thin-film electrode.

Before applying SWV for kinetic measurements, the response of the thin-film electrodes was thoroughly inspected by CV to examine its reproducibility and stability by repetitive cycling of the potential. Typical repetitive cyclic voltammograms corresponding to the transfer of Cl$^-$ ions are given in Fig. 6a. The stability of the system is obvious. As Cl$^-$ is present in both liquid phases, it is a transferring ion for both oxidative and reductive systems. The reduction of Lu[tBu$_4$Pc]$_2$ to Lu[tBu$_4$Pc]$_2^-$ is accompanied by the expulsion of Cl$^-$ from n-octanol, whereas the oxidation of Lu[tBu$_4$Pc]$_2$ to Lu[tBu$_4$Pc]$_2^-$ is accompanied by ingress of Cl$^-$ from water into the organic phase. The results in Fig. 6b show the quasireversible maxima measured by varying the

SW frequency and inspecting the net SW peak current of both oxidative (curve 1) and reductive (curve 2) systems. Both quasireversible maxima correspond to the transfer of Cl$^-$ ions. The two maxima have the same position showing the same apparent kinetics of the two systems. As the two electrochemical systems involve different electron transfer reactions, but the same ion transfer reaction, it is obvious that the latter is the rate-determining step. This is in accord with the previous results collected by studying the kinetics of ion transfers at the W|NB interface by means of thin-film electrodes [14–16].

Another important criterion showing whether the ion transfer is the rate-controlling step is based on the evolution of the quasireversible maximum with the concentration of the transferring ion in the aqueous phase. The theory has shown [15, 16] when the ion transfer is the rate-determining step, that the position of the quasireversible maximum shifts consistently with the ion concentration, toward higher critical frequencies when the concentration increases in the aqueous phase. The plot $\log(f_{max}^{-0.5})$ vs $\log(c_{An_{(w)}^-})$ is a line with a slope being dependent on the transfer coefficient. On the contrary, if the electron transfer at the EPPGE|OCT interface controls the rate of the overall process, the position of the maximum is insensitive to the concentration of the transferring ion [15]. The evolution of the quasireversible maxima with the concentration of the transferring ClO_4^- ion is presented in Fig. 7. The maximum strongly shifts toward higher critical frequencies by increasing the concentration of the ion, confirming clearly that the ion transfer is the rate-determining step. The inset in Fig. 7 shows a linear dependence between $\log(f_{max}^{-0.5})$ and $\log(c_{ClO_{4(w)}^-})$ with a slope of −0.63 (R=0.999). For the transfers of Cl$^-$ and NO$_3^-$, the corresponding slopes are −0.122 (R=0.999) and −0.476 (R=0.990), respectively (Table 3). All these data confirm that the ion transfer reaction at the W|OCT interface is the rate-determining step for all three studied anions. Experimental quasireversible maxima have been compared with the theoretical ones calculated on the basis of model presented in [15], and the standard rate constants have been estimated. All data referring to kinetic measurements are listed in Table 3.

Table 3 Analysis of the quasireversible maxima measured for three different concentrations of the transferring ion in the aqueous phase

Transferring ion	Critical frequency (f_{max}/Hz) for $c_{An_{(W)}}^* / mol\ l^{-1}$			$\log\left(f_{max}^{-1/2} / Hz^{-1/2}\right)$ vs $\log\left(c_{An_{(W)}}^* / mol\ l^{-1}\right)$	$10^4 \times k_s / cm\ s^{-1}$
	0.1	0.5	1		
Cl$^-$	20	30	35	$y=-0.1223x-0.7734$ (R=0.999)	1
ClO$_4^-$	7	50	130	$y=-0.6303x-1.0497$ (R=0.999)	3
NO$_3^-$	12	70	100	$y=-0.4758x-1.0271$ (R=0.990)	5

The other experimental conditions are the same as in Fig. 7. The standard rate constants have been estimated on the basis of the theoretical model presented in [15] using the critical frequencies measured for $c_{An_{(W)}}^* = 0.5\ mol/l$.

Conclusion

Three-phase and thin-film electrodes assembled by using EPPGE, *n*-octanol, and Lu[*t*Bu$_4$Pc]$_2$ are novel electrochemical tools to study both thermodynamics and kinetics of hydrophilic ion transfers across W|OCT interface. Versatile redox properties of Lu[*t*Bu$_4$Pc]$_2$ allow simultaneous inspection of both anion and cation transfers in a single voltammetric experiment. Thermodynamic measurements can be conducted with three-phase electrodes in the absence of any deliberately added supporting electrolyte in the organic phase. To the best of our knowledge, we reported on the first set of electrochemical experiments of alkali metal cation transfers from W to OCT, which enabled estimation of their Gibbs transfer energies. In a comparative study performed by using OCT, NB, and OCT–NB mixture as organic solvents, the strong affinity of OCT toward coordination of alkali metal cations has been confirmed. As a consequence, the transfer energies from W to OCT of strongly hydrophilic cations Li$^+$, Na$^+$, and K$^+$ are notably lower compared to W–NB system.

When suitable electrolytes are available to be dissolved in OCT, a thin-film electrode configuration can be utilized to assess the kinetics of the ion transfer across W|OCT interface. The proposed methodology, developed under conditions of SWV, provides kinetic information for the ion transfer across a nonpolarizable W|OCT interface, the potential of which is controlled by the transferring ion present in a large excess in both liquid phases. It has been demonstrated that this approach can be effectively applied to assess the kinetics of ClO$_4^-$, NO$_3^-$, and Cl$^-$ across W|OCT interface. The kinetic measurements of other ions have been prevented so far by the lack of suitable electrolytes soluble in OCT.

References

1. Reymond F (2001) In: Volkov AG (ed) Liquid interfaces in chemical, biochemical and pharmaceutical applications. Marcel Dekker, New York, pp 733
2. Zhao YH, Abraham MH (2005) J Org Chem 70:2633
3. Leo A, Hansch C, Elkins D (1971) Chem Rev 71:525
4. Girault HH, Schiffrin DJ (1989) In: Bard AJ (ed) Electroanalytical chemistry, vol 15. Marcel Dekker, New York, pp 1–141
5. Gulaboski R, Mirčeski V, Scholz F (2002) Electrochem Commun 4:277
6. Scholz F, Komorsky-Lovrić Š, Lovrić M (2000) Electrochem Commun 2:112
7. Komorsky-Lovrić Š, Riedl K, Gulaboski R, Mirčeski V, Scholz F (2002) Langmuir 18:8000
8. Gulaboski R, Galland A, Bouchard G, Caban K, Kretschmer A, Carrupt P, Stojek Z, Girault HH, Scholz F (2004) J Phys Chem B 108:4565
9. Bouchard G, Galland A, Carrupt P-A, Gulaboski R, Mirčeski V, Scholz F, Girault HH (2003) Phys Chem Chem Phys 5:3748
10. Scholz F (2006) Annu Rep Prog Chem C 102:43
11. Scholz F, Gulaboski R (2005) Faraday Discuss 129:169
12. Quentel F, Mirčeski V, L'Her M (2005) J Phys Chem B 109:1262
13. Quentel F, Mirčeski V, L'Her M, Mladenov M, Scholz F, Elleouet C (2005) J Phys Chem B 109:13228
14. Quentel F, Mirčeski V, L'Her M (2005) Anal Chem 77:1939
15. Mirčeski V, Quentel F, L'Her M, Pondaven A (2005) Electrochem Commun 7:1122
16. Gulaboski R, Mirčeski V, Pereira CM, Cordeiro MNDS, Silva AF, Quentel F, L'Her M, Lovric M (2006) Langmuir 22:3404
17. Pondaven A, Cozien Y, L'Her M (1992) New J Chem 16:711
18. L'Her M, Pondaven A (2003) In: Kadish KM, Smith KM, Guilard R (eds) The porphyrin handbook, vol 16, phtalocyanines: spectroscopic and electrochemical characterization. Academic Press, pp 177–170
19. Scholz F, Gulaboski R, Caban K (2003) Electrochem Commun 5:929
20. Lovrić M (2002) In: Scholz F (ed) Electroanalytical methods, guide to experiments and applications. Springer, Berlin Heidelberg New York, pp 111–133
21. De Ligny CL, Alfenaar M, Van Der Veen NG (1968) Rec Trav Chim Pays-Bas 87:585
22. Marcus Y (1997) Ion properties. Marcel Dekker, New York
23. Osakai T, Ogata A, Ebina K (1997) J Phys Chem B 101:8341
24. Mirčeski V (2004) J Phys Chem B 108:13719
25. Mirčeski V, Gulaboski R, Scholz F (2004) J Electroanal Chem 566:351